

Compton scattering studies of charge transfer in Fe-Ni-B amorphous alloys

This article has been downloaded from IOPscience. Please scroll down to see the full text article.

1992 J. Phys.: Condens. Matter 4 2735

(<http://iopscience.iop.org/0953-8984/4/10/033>)

View [the table of contents for this issue](#), or go to the [journal homepage](#) for more

Download details:

IP Address: 171.66.16.159

The article was downloaded on 12/05/2010 at 11:31

Please note that [terms and conditions apply](#).

Compton scattering studies of charge transfer in Fe–Ni–B amorphous alloys

A Andrejczuk†, L Dobrzyński†, E Żukowski†, M J Cooper†, S Hamouda‡ and J Latuszkiewicz§

† The Faculty of Physics, Warsaw University Branch, ul. Lipowa 41, 15–424 Białystok, Poland

‡ Department of Physics, University of Warwick, Coventry CV4 7AL, UK

§ ul. Borsucza 74, 05–807 Podkowa Leśna, Poland

Received 8 August 1991, in final form 27 November 1991

Abstract. The difference Compton profiles for amorphous alloys of composition $\text{Fe}_{82-x}\text{Ni}_x\text{B}_{18}$ ($x = 70, 41$ and 12) have been studied using 60 keV and 412 keV γ -radiation. The data have been analysed on the basis of the O'Handley and Boudreaux model, involving charge transfer from boron to transition metal 3d bands on alloying. This model, which is often invoked to explain the magnetic moment in these amorphous alloys, does not fit the measured Compton profiles and a simpler model, consistent with the experimental data, is considered. This is based simply on the free atom profiles of 3d states in nickel and iron with a small charge transfer from the conduction band to the nickel 3d states. Our data also show that the iron and nickel sites in these alloys are weakly ferromagnetic.

1. Introduction

1.1. Background work

The mechanism of magnetic moment formation in amorphous metals, and the general electronic structure of these materials, are not well understood. The magnetic moments of amorphous alloys are usually lower than the related crystalline materials which do not, of course, contain metalloid atoms such as boron, silicon or phosphorus. The complexity of the atomic arrangement in these systems creates considerable difficulty in the theoretical description of the electronic structure, magnetic moments, etc. The topic continues to be of considerable interest and further experimental evidence on the behaviour of the alloys is needed for a proper theoretical description. A study of the electron momentum distribution by Compton scattering is a particularly useful experimental method of investigating the behaviour of the outer electrons that determine magnetic properties [1].

In our previous Compton experiment [2] we studied a pseudobinary $(\text{Co,Ni})_{70}\text{Fe}_5\text{Si}_{15}\text{B}_{10}$ system in which the nickel atoms were believed to carry no magnetic moment or a very small one (less than $0.05\mu_B$ [3]). From the Compton profiles obtained it was inferred that, when nickel substitutes for cobalt, charge transfer from the conduction band to the 3d states takes place. Such a transfer could explain qualitatively the observed reduction of the magnetic moment on nickel. In

order to get more insight into that problem a much simpler system needed to be studied. Experimentally, however, there are some problems. In an experiment like ours [2] one compares the Compton profiles of samples with different compositions and when the alloy constituents are close to each other in the periodic table of elements, the composition difference must be quite pronounced to make the Compton profile changes clearly visible. In addition, rather large sample volumes are required and it is not always possible to make the amorphous ribbon of a given composition. Therefore in practice choice is strongly limited by the availability of the samples of interest. For these reasons the present studies concern quasibinary alloys $(\text{Fe,Ni})_{82}\text{B}_{18}$ in which the Ni to Fe ratio can rather easily be varied, and which contain only one metalloid element.

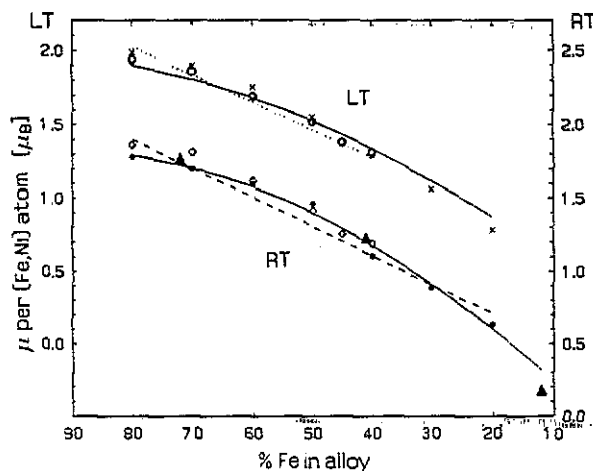


Figure 1. Magnetic moment per transition metal atom as a function of TM composition in $(\text{Fe,Ni})_{80}\text{B}_{20}$ alloys. Data at 0 K (LT): \circ , taken from [4]; and \times , taken from [5]. The dotted curve represents the fit based on fixed magnetic moments of iron and nickel [4]. The full curve fitted to the \circ points shows the variable moments predicted by equations (1) and (2). Data at room temperature (RT): \blacktriangle , magnetic moment measured on the $(\text{Fe,Ni})_{82}\text{B}_{18}$ samples used in these experiments; \bullet , taken from [5]; \diamond , taken from [4]. Our fit to the data of [5] with the fixed moments of Fe and Ni is depicted by the dashed curve. The full curve shows the variable TM moments fit.

The compositional variation of the average magnetic moment per transition metal atom (TM) is shown for $\text{Fe}_{80-x}\text{Ni}_x\text{B}_{20}$ in figure 1, which is taken from [4] and [5]. The authors of [4] concluded that this behaviour can be interpreted by assuming that iron contributes (at 0 K) $2.1\mu_B$ and nickel $0.6\mu_B$ while a decrease by $0.3\mu_B$ is associated with every boron atom. This leads to the straight line fit to the magnetisation data shown by the dotted line in figure 1. Apart from the flattening of the curve on the iron-rich side this interpretation is far from unique. One can get an equally good fit by assuming that the magnetic moments of iron and nickel are $1.99\mu_B$ and $0.67\mu_B$, respectively, ignoring the role of boron entirely.

The other possibility, discussed in [4], is the hypothesis that the magnetic moments of iron and nickel atoms in the amorphous alloys vary with the nickel concentration as in the crystalline $\text{Fe}_x\text{Ni}_{1-x}$ alloys, i.e.

$$\mu_{\text{Ni}} = 0.57 + 0.20x \quad (1)$$

$$\mu_{\text{Fe}} = 2.20 + 0.80(1 - x). \quad (2)$$

Furthermore the authors assumed that each boron atom reduces the Ni-Fe 'molecule' moment by $1.2\mu_{\text{B}}$. This fit to the experimental data is shown by the full curve in the upper part of figure 1. We see, however, that such a curve describes the data in a limited concentration range only.

Similar considerations can be made for the magnetic moments measured at room temperature [5] (see the lower plots in figure 1). For example, the linear fit gives magnetic moments of iron and nickel equal to $1.90\mu_{\text{B}}$ and $0.31\mu_{\text{B}}$, respectively. The variable moments can be expressed as: $\mu_{\text{Ni}} = -0.15 + 0.46x$ and $\mu_{\text{Fe}} = 1.79 + 0.98(1 - x)$. This means that the nickel moment is largely induced by its iron neighbours and there is no need to invoke any role for boron in these calculations. It is noteworthy that the coefficients of x and $(1 - x)$ are not unique; only their sum can be fitted unambiguously.

Unfortunately, these phenomenological descriptions provide no clues to the role played by boron atoms in the formation of individual magnetic moments on nickel and iron atoms. Therefore we focus our attention on the mechanism of magnetic moment formation rather than on the value of the moment itself.

1.2. Charge transfer and bonding models

There are two quite different explanations of the magnetic moments in the literature. On the one hand it is suggested that the metalloid atom directly donates electrons to the d-band of the TM matrix, thereby reducing the moments and leaving a charged boron ion. The charge transfer required to produce the observed moments on the TM atoms can then be calculated. On the other hand the effect of boron, silicon or phosphorus can be considered in terms of a covalent bonding interaction with the TM which alters the width and relative energies of the majority and minority bands in a manner that reduces the TM moments.

It is interesting to consider what happens in nickel-iron alloys in which the nickel magnetic moment is believed to be non-zero, as in the Fe-Ni-B alloys containing 18 at.% of boron investigated in this work. Alloys of this kind (actually containing 20 at.% of boron) have been studied by Becker *et al* [4] and O'Handley and co-workers [5, 6, 7].

A comprehensive discussion on the hybridisation of metalloid s- or p-like levels with TM d-bands and on the charge transfer phenomena can be found in the papers by O'Handley [6, 7]. In these, it is pointed out that the s-d charge transfer between TM can be preceded by an electron transfer from the metalloid atom to the localised d-bands of the TM atoms. The amount of this charge transfer depends on both the specific metalloid atom (e.g. B, Si or P) and the nature of the TM matrix. For 20 at.% of boron it is estimated [6], that each boron atom transfers effectively 1.4 electrons to the nickel matrix, i.e. the number of 3d electrons is increased by approximately 0.35 per nickel atom. (Please note that in the rigid band model of the TM matrix the charge transfer was estimated as 1.6 electrons per boron atom [5].) It should be stressed that an important assumption by the authors of [6] is that the Fermi level lies above the minority spin band (i.e. strong ferromagnetism) at least at nickel sites. If all the transferred electrons fill up the minority spin states only, then the magnetic moment on nickel must be reduced from the original value of $0.6\mu_{\text{B}}$ to $0.25\mu_{\text{B}}$. In accordance with this model [6] μ_{Ni} is independent of concentration in $(\text{Fe,Ni})_{80}\text{B}_{20}$ alloys, which evidently contradicts the model described by equations (1) and (2).

The charge transfer to a cobalt matrix is supposed to be 1.6 electrons per boron atom and to iron it is as high as 2.2–2.4 electrons. In the latter case, however, the relation between the charge transfer and the magnetic moment is more complicated as iron sites in the iron-rich alloys are considered as weakly ferromagnetic (holes exist in both subbands). The authors of [6] assume that the iron moment increases with the nickel content.

As was mentioned in section 1.1, our previous [2] Compton profile studies on pseudobinary (Co,Ni)-amorphous alloys concluded that addition of nickel results in charge transfer from the conduction band, presumably to the Ni 3d band. The possibility of charge transfer from the metalloid atom was not considered. These studies, however, could hardly provide a critical test of charge transfer from boron for two reasons. Firstly, the predictions of O'Handley are similar for transfers to Co and Ni, and secondly, the situation was complicated by the presence of silicon as well as boron. (Yamauchi and Mizoguchi [8] have shown that the moment reduction due to Si is twice that associated with B.) The simpler Fe–Ni–B alloys studied here are expected to provide a much more sensitive and unambiguous test because of the predicted large difference in charge lost by boron to Fe (2.2–2.4 electrons) and Ni (1.4 electrons).

A much more drastic reduction of the nickel magnetic moment than the iron one in amorphous alloys is also clearly predicted in the X- α cluster calculations by Messmer [9]. This work, also cited and discussed by O'Handley [7], favours s-d/p-d hybridisation between boron and the transition elements (Fe,Ni) as the mechanism responsible for the d-moment reduction. This work is of special relevance to this study because the calculation was performed for the cluster composition Fe₂Ni₂B which is close to the one studied here. The main result of Messmer's calculation is a substantial broadening of the 3d bands due to the presence of boron atoms and a strong preference of boron to bond covalently with nickel.

The theoretical considerations described above are much more qualitative than quantitative. The assumptions underlying the models used can be questioned and in this situation the consideration of additional data to the measured magnetic moments is strongly recommended.

1.3. Strong or weak ferromagnetism

The theoretical attempts to describe the concentration dependence of the mean magnetic moment observed in the alloys of interest rely heavily on assumptions concerning the kind of band ferromagnetism exhibited by iron and nickel. For example, O'Handley and Boudreaux [6] assumed that nickel shows strong ferromagnetism while iron in the iron-rich sample exhibits weak ferromagnetism. At higher nickel concentrations iron tends to the strong ferromagnetism case.

The magnetisation versus temperature measurements carried out by Babič *et al* [10] on Fe_xNi_{80-x}B₁₈Si₂ and Fe₈₀B₂₀ samples gave support to the concept of strong ferromagnetism of iron. However, the theoretical analysis of magnetic moments in Fe_{1-x}B_x systems, carried out by Malozemoff *et al* [11] and justifying the idea of so-called magnetic valence, concluded that these alloys represent rather weak ferromagnetism. The magnetoresistivity measurements of Fe_xNi_{80-x}B₂₀ [12] gave evidence for weak ferromagnetism of these alloys, although the authors state that Fe₈₀B₂₀ is on the verge of becoming a strong ferromagnet. At the same time, they supported O'Handley and Boudreaux's [6] concept of charge transfer from metalloid atoms to the 3d bands. Spin-polarised photoemission studies [13] seem also to favour

weak ferromagnetism at low nickel concentrations and are in agreement with the idea of [6] that at high nickel concentrations there is a tendency towards strong ferromagnetism.

As is seen, the experiments cited above do not lead to a definite conclusion concerning the type of band ferromagnetism involved. We shall show that our data support the model of weak ferromagnetism.

1.4. Compton scattering measurements

The quantity measured in these experiments is the spectral distribution of the Compton scattered gamma radiation. Under conditions of high energy transfer the scattering can be considered in an impulse approximation with the result that the scattering cross-section is proportional to $J(p_z)$, with the integral of the electron momentum density, $n(\mathbf{p})$, over the two momentum components perpendicular to the scattering vector (assumed to point along the z -direction):

$$J(p_z) = \iint n(\mathbf{p}) dp_x dp_y. \quad (3)$$

This expression implies certain simplifying assumptions about the relativistic cross-section for scattering from a moving electron [14]; the approximations adopted have been validated in numerous other Compton scattering studies (for example [15, 16]).

If a γ -ray source with a photon energy of several hundreds of keV (^{198}Au : 412 keV; ^{137}Cs : 662 keV) is used for Compton scattering experiments at large angles of scattering the energy transferred also amounts to hundreds of keV and the impulse approximation will be valid for all the bound electrons. In the case of a softer radiation, e.g. 59.54 keV γ -rays from a ^{241}Am source, the energy transfer is typically 12 keV and the impulse approximation will not be valid for the K-shell electrons. Fortunately this has little influence on the consideration of Compton profile differences since the core contributions cancel. This situation is well known and is discussed elsewhere (e.g. [17]). This approach has been used successfully in numerous studies of anisotropy in TM and TM alloys [18, 19] and is explained in our earlier study [2].

2. The experiments

Measurements are reported for the two samples of $\text{Fe}_{82-x}\text{Ni}_x\text{B}_{18}$ alloys, with $x = 70$ (sample S1) and $x = 12$ (sample S2), which were prepared in the form of ribbons of width 11–12 mm and thickness 20–30 μm by rapid quenching on a copper roller. (Studies on the intermediate composition, $x = 41$ (sample S3), have been made and the results are consistent with those obtained in the study of the samples with the extreme compositions considered here.) The densities have been estimated from calculations based on the atomic radii and the packing fraction as described in the paper by Dobrzyński *et al* [3].

Two γ -ray sources, in different locations, were used: a 120 Ci ^{198}Au source in Białystok and a 5 Ci ^{241}Am source at Warwick [20]. The gold isotope has the advantage of affording the higher resolution but its half-life is only 2.7 days (cf. 458 years for americium) and costly irradiations must be made to replenish the material. The gold source spectrometer is a new instrument, similar to ones previously operated elsewhere (see e.g. [21, 22]) and will be described in a separate publication [23]. Both

instruments use Ge semiconductor detectors to analyse the scattered radiation. Their limited energy resolution, coupled with the contribution from the divergence of the incident and scattered beams, leads to instrument resolutions of 0.40 and 0.57 atomic units of momentum for the ^{198}Au and ^{241}Am spectrometers, respectively. (Note, 1 au corresponds to an electron momentum of 1.99×10^{-24} m kg s $^{-1}$; electrons at the Fermi surface of aluminium, for example, have a momentum of 0.926 au.)

Many energy-dependent corrections are involved in the data processing. For example those associated with absorption and multiple scattering in the sample and the detector efficiency. However their influence on the final difference profiles can be minimised if the samples are identical in size. Therefore the ribbons were cut into smaller pieces and clamped together, so as to form samples with a square cross-section of approximately 24 mm \times 24 mm and thickness 1 mm. The count rate in the americium experiment was about 30 counts per second under the Compton peak. No contribution from the holder could be detected in the measurements with either spectrometer. In any event any such scattering, together with other parasitic systematic effects would cancel in the differences formed from measurements on the samples.

Electronic drift was checked by monitoring the position of the 122 keV line from a ^{57}Co calibration source in the ^{198}Au experiment and the elastic line in the ^{241}Am spectrometer. Incomplete charge collection in the detector is largely responsible for the asymmetry in the measured Compton spectra (the Compton profile, as defined by equation (3) must, of course, be symmetric). As is usual in line shape analyses of this kind only the high energy side of the profiles which are relatively free from these effects, were processed. A summary of the experimental details is compiled in table 1. The magnetic moments measured at room temperature with a magnetic balance are also shown in figure 1. As can be seen, our data agree well with the values taken from measurements made on $(\text{Fe,Ni})_{80}\text{B}_{20}$ samples. Therefore the previous theoretical analysis of the magnetic moments of $(\text{Fe,Ni})_{80}\text{B}_{20}$ should apply to $(\text{Fe,Ni})_{82}\text{B}_{18}$ as well.

Table 1. Experimental details.

Sample	μ per TM at room temperature (μ_B)	Measurement time (hours)	Integrated Compton (counts)	Calculated density \dagger ($\text{kg m}^{-3} \times 10^{-3}$)
S1				
$\text{Fe}_{12}\text{Ni}_{70}\text{B}_{18}$	0.18	258	2.4×10^7	7.98
		159 ‡	0.8×10^6	
S2				
$\text{Fe}_{70}\text{Ni}_{12}\text{B}_{18}$	1.77	288	3.0×10^7	7.43
		161 ‡§	1.1×10^6	
S3				
$\text{Fe}_{41}\text{Ni}_{41}\text{B}_{18}$	1.23	273	3.1×10^7	7.70

† Packing fraction 0.697 was taken from reference [24] where a number of various amorphous alloys densities have been analysed.

‡ From measurements made on the ^{198}Au spectrometer. Two gold sources (one per sample), activated to about 100 Ci, have been used.

§ In this measurement the thickness of sample S2 was 1.8 mm. This was reduced later to the standard value of 1 mm used in all the other measurements.

3. Data processing

The data processing routines which involve the corrections for background, detector response function, Compton cross-section and multiple-scattering, are standard and identical to those described in an earlier paper [2]. In spite of the poorer statistics in the high energy study, the Compton profiles measured in both research centres are similar. In view of the greater statistical accuracy of the americium data the results from the gold spectrometer will only be used for a qualitative comparison with the data from the ^{241}Am spectrometer. (Since this experiment the performance of the Compton spectrometer in Białystok has substantially improved—see Andrejczuk *et al* [23].)

The positive momenta data have been used to form the difference profile S1-S2. The free atom core ($1s^2 2s^2 2p^6 3s^2 3p^6$) profiles [25] corresponding to the appropriate Fe/Ni compositions had been convoluted with a Gaussian of FWHM equal to the resolution of the experiment and subtracted from each profile. The necessary corrections for K-shell binding edge discontinuities in Fe and Ni were made. The resulting profiles contain the contribution of residual 3d and 4s electrons in iron and nickel. The difference profile, $\Delta J_{3d,4s}$, shows the changes associated with the different (3d, 4s) band configurations when nickel is substituted for iron. These results are reproduced in figure 2 as full and open circles, respectively for the measurements made on the americium and gold spectrometers. The area of the $\Delta J_{3d,4s}$ (S1-S2) curve (p_z from 0 au to 7 au) is equal to 0.55 electrons. This reflects the increase in the number of electrons per formula unit (in the measured momentum range) in $J(\text{S1})_{3d,4s}$ by comparison to the $J(\text{S2})_{3d,4s}$ profile.

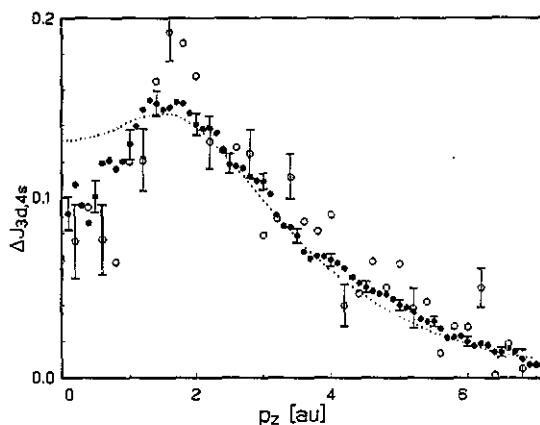


Figure 2. The processed difference Compton profiles $\Delta J_{3d,4s}$. ●, represent the measurements made on the ^{241}Am spectrometer for the S1-S2 samples. ○, show the same difference measured on the ^{198}Au spectrometer. The 3d free-atom Compton profiles for nickel and iron have been used to plot (dotted curve) the 3d difference profile for S1-S2 samples.

4. Data analysis

Previous studies of the transition metal difference Compton profile [2] showed that

when no electronic band structure calculations are available, free atom tabulated d-electron profiles are reasonable starting points to analyse the experimental difference $\Delta J_{3d,4s}$. One-electron 3d (free atom) profiles for Fe, $\{3d\}_{\text{Fe}}$, and Ni, $\{3d\}_{\text{Ni}}$, have been used to model the experimental difference profile $\Delta J_{3d,4s} = D[8\{3d\}_{\text{Ni}} - 6\{3d\}_{\text{Fe}}]$, where D is the difference in nickel/iron content between the pair of samples. Identical free-electron-like 4s configurations in Ni and Fe were assumed; thus there is no contribution from these electrons to ΔJ . This free atom difference for $D = 0.58$ is plotted as a dotted curve in figure 2. Inspection of the data confirms that the difference 3d atomic profile is a good initial approximation for modelling the experimental results. It reproduces the measurements very well for momenta with $p_z > 2$ au, but a discrepancy is evident at lower momenta.

In the following paragraphs the experimental results will be analysed on the basis of two charge-transfer models. Firstly, the O'Handley and Boudreaux model [6] involving boron outer electrons and, secondly, a simple model considering TM sites only.

In order to avoid ambiguities associated with different definitions of charge transfer, the basis of our calculations is set out as follows. Let us express the sample composition as $\text{Fe}_a\text{Ni}_b\text{B}_c$ and the (3d, 4s) bands configuration as $3d^m4s^{8-m}$ for iron and $3d^n4s^{10-n}$ for nickel. In the O'Handley and Boudreaux model, formulated in section 1.2, it was assumed that $m = 7.05$ and $n = 9.4$, and that every boron atoms donates $r = 1.4$ electrons to nickel and $s = 2.3(1)$ electrons to iron atoms on alloying. The difference profile can be expressed in a similar form to that used above for the free atom difference, i.e.

$$\Delta J_{3d,4s} = D[(n + \Delta n)\{3d\}_{\text{Ni}} - (m + \Delta m)\{3d\}_{\text{Fe}} + (\Delta m - \Delta n)\{2s2p\}_{\text{B}} + (m + 2 - n)\{\text{FE}\}] \quad (4)$$

where $\{\text{FE}\}$ is a TM free-electron profile, $\{2s2p\}_{\text{B}}$ is the Compton profile of the outer boron shell, Δn is the number of electrons transferred from boron atoms to the 3d nickel band and Δm is an equivalent transfer from boron to the 3d band of iron.

Within the model of [6] $\Delta n = cr/(a + b)$ electrons while $\Delta m = cs/(a + b)$ electrons. This results in a total charge transfer per boron atom of 1.53(2) and 2.17(9) electrons for the S1 and S2 samples, respectively. The results of the calculations based strictly on the above values of r and s given by O'Handley and Boudreaux [6] are shown in figure 3 by the dotted curves. This model require a charge transfer of $\Delta n \simeq 0.31$ and $\Delta m \simeq 0.50(2)$ electrons to TM 3d sites and gives a contribution of $D(\Delta m - \Delta n) \simeq 0.11$ electrons from the boron $\{2s2p\}_{\text{B}}$ shell (see the free-electron-like profile depicted by the dashed curve, figure 3). Simultaneously, the reduction in the number of electrons in the TM 4s band is equal to $D(m + 2 - n) \simeq -0.20$ electrons. Hence the effective decrease in the total number of free electrons is estimated as 0.09 electrons. Their Compton profile is shown as the dotted curve in the lower part of figure 3. The agreement with experiment is rather poor. There is obviously a need to improve the model.

Let us note that, because the outer electron configuration of boron is $2s^22p^1$, for charge transfers from boron larger than 1 electron (as calculated above) the term $\{2s2p\}_{\text{B}}$ in equation (4) will contain the Compton profile of 2s electrons only. In our experiments this profile is practically indistinguishable from the free-electron TM profile (the last term in equation (4)). Therefore, the experimentally determined difference $\Delta J_{3d,4s}$ is described effectively by only 2 parameters: n_{tot} and m_{tot} , thus

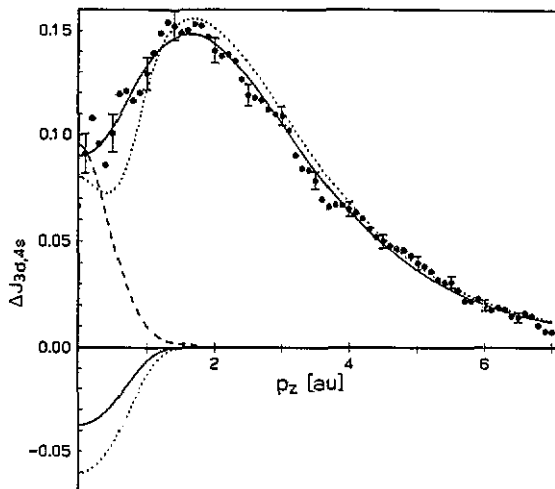


Figure 3. The best fits to the S1-S2 difference data (●) measured on the ^{241}Am spectrometer. The dotted curve represents the calculations based strictly on the O'Handley charge transfer model. The contribution of boron outer electrons is shown by the dashed curve. The fits from the modified O'Handley model and the model involving the 4s-3d charge transfer between Ni and Fe atoms only are plotted as a full curve. The curves at the bottom show the negative free-electron Compton profiles indicating the additional charge transfer to the 3d band when nickel is substituted for iron.

equation (4) becomes

$$\Delta J_{3d,4s} = D\{n_{\text{tot}}\{3d\}_{\text{Ni}} - m_{\text{tot}}\{3d\}_{\text{Fe}} + (m_{\text{tot}} + 2 - n_{\text{tot}})\{\text{FE}\}\} \quad (5)$$

where $n_{\text{tot}} = n + \Delta n$ and $m_{\text{tot}} = m + \Delta m$ are the total number of 3d electrons in nickel and iron, respectively.

The best agreement with experiment is obtained for $n_{\text{tot}} \simeq 9.0(1)$ and $m_{\text{tot}} \simeq 6.9(1)$. The effective change in the number of conduction electrons is $D(m_{\text{tot}} + 2 - n_{\text{tot}})$. In practice it is determined more accurately from a fit of the free-electron profile; the value obtained is $-0.05(1)$. This implies a transfer of conduction electrons to the 3d band in TM. The calculated curves are shown in figure 3 by the full curves.

Information on the source of the transferred electrons is lost in equation (5), therefore the alternative approach (which we now describe) is to assume that boron is not involved in charge transfer at all. Only the 4s electrons in TM fill the 3d band in nickel (as necessary) when nickel is substituted for iron. Within this model equations (4) and (5) are equivalent and calculations are represented by *exactly the same full curves* in figure 3.

The above analysis can be used to discuss the magnetic moments measured on the samples under consideration. The number of 3d electrons on nickel (9.0) is such that if it represented a strong ferromagnetism case over the whole concentration range (70-12 %Fe), its magnetic moment would have to be as high as $1.0\mu_{\text{B}}$. There is no evidence to support this. In fact, experiments indicate that μ_{Ni} is close to, or below, $0.2\mu_{\text{B}}$, which implies that nickel represents weak ferromagnetism. Moreover, the fact that in these amorphous alloys n_{tot} is lower than in the crystalline case (9.0 compared to 9.4) contradicts the idea of the charge transfer from boron to nickel. Indeed, a transfer in the opposite direction would explain the values obtained

even better. The value of m_{tot} for the iron site also does not confirm a charge transfer from boron, assuming 3d band occupation in the crystalline phase proposed by O'Handley and Boudreaux (6.9 compared to 7.05). At the same time, the possible values of iron magnetic moments below $2.5\mu_{\text{B}}$, indicate that iron also represents a weak ferromagnetism case.

The necessity of introducing a small negative contribution from conduction electrons shows that each nickel atom adds fewer conduction electrons than each iron atom does, or that under alloying with nickel some conduction electrons are transferred to the Ni 3d-band.

5. Conclusions

The model of charge transfer from boron to TM, as exactly proposed by O'Handley and co-workers [6, 7] is in disagreement with the Compton profile data. The analysis of the possible electron configuration of iron and nickel in the alloys studied show that the filling of the 3d bands ($n_{\text{tot}} = 9.0$ and $m_{\text{tot}} = 6.9$) is lower than assumed in [6] ($9.4 + 0.31$ and $7.05 + 0.50$, respectively). Therefore any charge transfer from boron to TM would require even lower initial numbers of d-electrons on Ni and Fe atoms.

The experimental difference profile $\Delta J_{3d,4s}$ can be simply explained ignoring the role of boron as a source of additional electrons. Assuming free-atom configurations one would expect that substitution of iron by nickel should increase 3d band occupation by 2 electrons. The value obtained from statistical fits is 0.05(1) electrons greater and can be explained as due to an additional electron transfer from the 4s states. The same effect was previously seen in [2].

In order to reconcile the number of d-electrons for nickel and iron with the magnetic moments of the atoms, both kinds of atoms must represent weak ferromagnetism. This agrees well with the results of [11, 12, 13].

The non-linear variation of the mean magnetic moments of alloys with the nickel concentration shows that the individual magnetic moments of nickel and iron must be composition-dependent and that local-environment effects which can alter the exchange-splitting or deform the electronic density-of-states curves, should take place.

In order to have a better idea about the magnetic moment distribution in our alloys we plan to carry out magnetic x-ray absorption measurements of the near edge structure [26] at both Ni and Fe sites and measure *magnetic* Compton profiles in these alloys using elliptically polarised synchrotron radiation sources in an attempt to determine the respective moments.

Note added in proof. Cowley et al [27] have recently measured polarized neutron scattering on $(\text{Fe}_x\text{Ni}_{1-x})_{78}\text{B}_{12}\text{Si}_{10}$. They conclude that Ni magnetic moments are comparable with those of iron, but that the nickel moment is randomly oriented, so it does not contribute to the aligned moment. Again, this disagrees with the O'Handley and Boudreaux [6] charge transfer model and gives room for the relatively low value of n_{tot} obtained by us.

Acknowledgments

The authors are grateful to the SERC for the provision of a research fellowship (EZ), the British Council for travel grants (MJC), to A Malinowski for providing the sample

magnetisation data and to the University of Warsaw, College at Białystok for travel grants and hospitality during visits by MJC and EŻ.

References

- [1] Cooper M J 1985 *Rep. Prog. Phys.* **48** 415
- [2] Żukowski E, Dobrzyński L, Cooper M J, Timms D N, Holt R S and Latuszkiewicz J 1990 *J. Phys.: Condens. Matter* **2** 6315
- [3] Dobrzyński L, Szymański K, Waliszewski J, Malinowski A, Wiśniewski A, Baran M and Latuszkiewicz J 1990 *J. Magn. Magn. Mat.* **88** 23
- [4] Becker J J, Luborsky F E and Walter J L 1977 *IEEE Trans. Magn.* **MAG-13** 988
- [5] O'Handley R C, Hasegawa R, Ray R and Chou C-P 1976 *Appl. Phys. Lett.* **29** 330
- [6] O'Handley R C and Boudreaux D S 1978 *Phys. Status Solidi (a)* **45** 607
- [7] O'Handley R C 1983 *Amorphous Metallic Alloys* ed F E Luborsky (London: Butterworths) pp 257-82
- [8] Yamauchi K and Mizoguchi T 1975 *J. Phys. Soc. Japan* **39** 541
- [9] Messmer R P 1981 *Phys. Rev. B* **23** 1616
- [10] Babič E, Marohnič Ž and Wohlfarth E P 1983 *Phys. Lett.* **95A** 335
- [11] Malozemoff A A, Williams A R and Moruzzi V L 1984 *Phys. Rev. B* **29** 1620
- [12] Kaul S N and Rosenberg M 1983 *Phys. Rev. B* **27** 5698
- [13] Hopster H, Kurzawa R, Raue R, Schmitt W, Güntherodt G, Walker K H and Güntherodt H J 1985 *J. Phys. F: Met. Phys.* **15** L11
- [14] Ribberfors R 1975 *Phys. Rev. B* **12** 2067
- [15] Rollason A J, Schneider J R, Laundry D S, Holt R S and Cooper M J 1987 *J. Phys. F: Met. Phys.* **17** 1105
- [16] Rollason A J, Holt R S and Cooper M J 1983 *J. Phys. F: Met. Phys.* **13** 1807
- [17] Weiss R J, Cooper M J and Holt R S 1977 *Phil. Mag.* **36** 193
- [18] Timms D N, Brahmia A, Cooper M J, Collins S P, Hamouda S, Laundry D, Kilbourne C and Saint Lager M-C 1990 *J. Phys.: Condens. Matter* **2** 3427
- [19] Timms D N, Cooper M J, Holt R S, Itoh F, Kobayasi T and Nara H 1990 *J. Phys.: Condens. Matter* **2** 10517
- [20] Cooper M J, Holt R S and DuBard J L 1978 *J. Phys. E: Sci. Instrum.* **11** 1145
- [21] Holt R S, Cooper M J, DuBard J L, Forsyth J B, Jones T J L and Knight K M 1979 *J. Phys. E: Sci. Instrum.* **12** 1148
- [22] Pattison P and Schneider J R 1979 *Nucl. Instrum. Methods* **158** 145
- [23] Andrejczuk A, Dobrzyński L and Żukowski E *Nucl. Instrum. Methods* submitted
- [24] Kaul S N 1983 *Phys. Rev. B* **27** 5761
- [25] Biggs F, Mendelsohn L B and Mann J B 1975 *At. Data Nucl. Data Tables* **16** 201-309
- [26] Collins S P, Cooper M J, Brahmia A, Laundry D and Pitkanen T 1989 *J. Phys.: Condens. Matter* **1** 323
- [27] Cowley R A, Patterson C, Cowlam N, Ivison P K, Martinez J and Cussen L D 1991 *J. Phys.: Condens. Matter* **3** 9521